J Solid State Electrochem (2009) 13:1381–1386
DOI 10.1007/s10008-008-0695-z

ORIGINAL PAPER

Improvement of high-voltage cycling behavior of $Li(Ni_{1/3}Co_{1/3}Mn_{1/3})O_2$ cathodes by Mg, Cr, and Al substitution

Ling Liu · Kening Sun · Naiqing Zhang · Tongyong Yang

Received: 8 July 2008 / Revised: 4 September 2008 / Accepted: 29 September 2008 / Published online: 21 October 2008

Abstract To improve the electrochemical properties of $Li[Ni_{1/3}Co_{1/3}Mn_{1/3}]O_2$ at high charge end voltage (4.6 V), a series of the mixed transition metal compounds, $Li(Ni_{1/3}Co_{1/3-x}Mn_{1/3}M_x)O_2$ (M = Mg, Cr, Al; x=0.05), were synthesized via hydroxide coprecipitation method. The effects of doping Mg, Cr, and Al on the structure and the electrochemical performances of $Li[Ni_{1/3}Co_{1/3}Mn_{1/3}]O_2$ were compared by means of X-ray diffraction (XRD), scanning electron microscopy (SEM), galvanostatic charge–discharge tests, and electrochemical impedance spectroscopy. The XRD results show that all the samples keep layered structures with R3m space group as the $Li[Ni_{1/3}Co_{1/3}Mn_{1/3}]O_2$. SEM images show that all the compounds have spherical shapes and the Cr-doped sample has the largest particle size. Furthermore, galvanostatic charge–discharge tests confirm that the Cr-doped electrode shows improved cycling performance than the undoped material. The capacity retention of $Li(Ni_{1/3}Co_{1/3-0.05}Mn_{1/3}Cr_{0.05})O_2$ is 97% during 50 cycles at 2.8~4.6 V. The improved cycling performance at high voltage can be attributed to the larger particle size and the prevention of charge transfer resistance (R_{ct}) increase during cycling.

Keywords Lithium ion battery · $Li[Ni_{1/3}Co_{1/3}Mn_{1/3}]O_2$ · Cycling performance · High voltage · Doping

L. Liu · T. Yang
Department of Applied Chemistry, Harbin Institute of Technology, Harbin 150001, People's Republic of China

K. Sun (✉) · N. Zhang
Science Research Center, Harbin Institute of Technology, Harbin 150001, People's Republic of China
e-mail: sunkn@hit.edu.cn

Introduction

$LiCoO_2$ has been used as a major cathode material for lithium ion secondary battery because of its ease of production, high specific capacity, and good cycling performance. However, its high cost and toxicity limit its further use in newly developed multifunctional portable devices and electric vehicle systems [1–3]. Thus, extensive research has been carried out to find alternative cathode materials, such as $LiNiO_2$, $LiMn_2O_4$, $LiMnO_2$, and $LiFePO_4$. Although there has been a lot of progress in making these materials comparable to $LiCoO_2$ in many aspects, they still present various problems for practical applications.

Recently, layered $LiNi_xCo_{1-2x}Mn_xO_2$ has been synthesized by substituting electrochemically active metal like Ni and Mn at the Co site in $LiCoO_2$. Among all these materials, $Li[Ni_{1/3}Co_{1/3}Mn_{1/3}]O_2$ has attracted more attention because of its low cost, higher reversible capacity, and milder thermal stability [4–6]. Besides all the above merits, the cycling performance at high-voltage region is the most important property for high-power applications, such as electric vehicles, hybrid electric vehicles, and zero emission vehicles [7–9]. For $Li[Ni_{1/3}Co_{1/3}Mn_{1/3}]O_2$ cathode material, the cycling stability is undesirable, especially if cycled above 4.6 V.

In order to improve the cycling performance of $Li[Ni_{1/3}Co_{1/3}Mn_{1/3}]O_2$ at high voltage, we want to find a cation which is stable when it is charged to the high voltage. Mg^{2+}, Cr^{3+}, and Al^{3+} all have stable state when they are charged to 4.6 V, so we choose these three cations as the doping cations. In this paper, the $Li(Ni_{1/3}Co_{1/3-x}Mn_{1/3}M_x)O_2$ (M = Mg, Cr, Al; x=0, 0.05) compounds were prepared by a hydroxide coprecipitation method, and their structural, morphological, and electrochemical properties were discussed.

Experimental

Synthesis procedure

$(Ni_{1/3}Co_{1/3-x}Mn_{1/3}M_x)(OH)_2$ (M = Mg, Cr, Al; x=0, 0.05) powders were synthesized by hydroxide coprecipitation method. An aqueous solution of $NiSO_4 \cdot 6H_2O$, $CoSO_4 \cdot 7H_2O$, $MnSO_4 \cdot H_2O$, and M ($MgSO_4 \cdot H_2O$, $Cr(NO_3)_3 \cdot 9H_2O$, $Al(NO_3)_3 \cdot 3H_2O$) with a concentration of 1 mol L^{-1} was pumped into a continuously stirred tank reactor under nitrogen atmosphere. At the same time, NaOH solution of 2 and 0.36 mol L^{-1} of NH_4OH were also separately fed into the reactor. The solution was maintained at 50 °C with continuous stirring for 24 h and the pH value of the solution was carefully controlled at 12±0.02. The precipitated powder was filtered and washed, and then it was dried in a vacuum chamber at 80 °C for 12 h.

The obtained $(Ni_{1/3}Co_{1/3-x}Mn_{1/3}M_x)(OH)_2$ was mixed with a stoichiometric amount of $LiOH \cdot H_2O$ and ball-milled for 24 h. Then, the mixtures were calcined at 500 °C for 5 h. The final $Li(Ni_{1/3}Co_{1/3-x}Mn_{1/3}M_x)O_2$ powder was obtained after the last calcination at 900 °C for 12 h. All the procedures were carried out in air atmosphere.

Measurements

Powder X-ray diffraction (XRD) data were collected on a Rigaku D/max-$\gamma\beta$ diffractometer with CuKα radiation in the range of 10~80° (2θ). The surface morphology and particle size of the $Li(Ni_{1/3}Co_{1/3-x}Mn_{1/3}M_x)O_2$ compounds were observed with a scanning electron microscope using a HITACHI-S4700 field emission microscope with an acceleration voltage of 2.0 kV.

The charge–discharge tests were carried out using a CR2025 coin-type cell, which consists of a cathode and a lithium metal anode separated by a Celgard 2400 porous polypropylene film. The cathodes were prepared by blending $Li(Ni_{1/3}Co_{1/3-x}Mn_{1/3}M_x)O_2$ powder, carbon black, and polyvinylidene difluoride (8:1:1 mass) in n-methyl pyrrolidone. The obtained slurry was pasted on Al foil. The electrolyte was 1 M $LiPF_6$ with 1:1 (volume) ethylene carbonate–ethyl-methyl carbonate, and lithium metal was used as the anode. The cells were assembled in an argon-filled glove box and tested at a rate of 32 mA g^{-1} (0.2 C) between 2.8 and 4.6 V. Electrochemical impedance spectroscopy (EIS) measurement was carried out with a PARSTAT 2273 advanced electrochemical system at room temperature using 10 mV ac voltage signal in the frequency range of 1 MHz to 10 mHz. During the EIS testing for the coin cells, the lithium metal anode was used as the reference and counter electrodes.

Results and discussion

The X-ray diffraction patterns of $Li(Ni_{1/3}Co_{1/3-x}Mn_{1/3}M_x)O_2$ (M = Mg, Cr, Al; x=0, 0.05) are shown in Fig. 1. All peaks in each pattern can be indexed based on a hexagonal α-$NaFeO_2$ structure with R3m space group (No. 166). It is observed that phase-pure layered structure with no remarkable secondary phase has been formed for all materials except Al-doped material. The $LiAlO_2$ impurity phase was present in the Al-doped sample. In the XRD patterns, integrated peak splits of (006)/(102) and (018)/(110) were known to be an indicator of characteristic of layered structure like $LiNiO_2$ and $LiCoO_2$ [10, 11]. As can be seen in Fig. 1, the (006)/(102) and (018)/(110) peaks are all clearly split, which indicates the highly ordered layered structure of the prepared $Li[Ni_{1/3}Co_{1/3}Mn_{1/3}]O_2$.

We calculated the lattice parameters of the powders by a least-square method from the results of Fig. 1. The lattice parameters of a, c, and c/a and the volume of unit cell are summarized in Table 1. The lattice parameters of $Li(Ni_{1/3}Co_{1/3}Mn_{1/3})O_2$ match well with the values observed by other researchers [12, 13]. As seen from Table 1, the parameters of a and c and the cell volume increased in the cases of $Li(Ni_{1/3}Co_{1/3-0.05}Mn_{1/3}Mg_{0.05})O_2$ and $Li(Ni_{1/3}Co_{1/3-0.05}Mn_{1/3}Cr_{0.05})O_2$ which should be related to the larger radii of Mg^{2+} (0.78 Å) and Cr^{3+} (0.62 Å) than that of Co^{3+} (0.54 Å). On account of the size of Al^{3+} (0.53 Å) which is close to that of Co^{3+} (0.54 Å), the parameters of $Li(Ni_{1/3}Co_{1/3-0.05}Mn_{1/3}Al_{0.05})O_2$ were nearly unchanged.

Figure 2 shows the morphologies and the particle size of $Li(Ni_{1/3}Co_{1/3}Mn_{1/3})O_2$ and $Li(Ni_{1/3}Co_{1/3-0.05}Mn_{1/3}M_{0.05})$

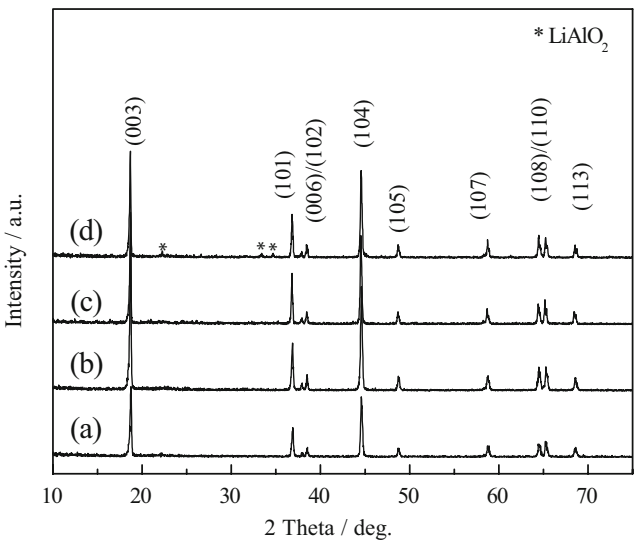

Fig. 1 XRD patterns of $LiNi_{1/3}Co_{1/3-x}Mn_{1/3}M_xO_2$ (M = Mg, Cr, Al, x=0, 0.05): (*a*) $LiNi_{1/3}Co_{1/3}Mn_{1/3}O_2$, (*b*) $LiNi_{1/3}Co_{1/3-0.05}Mn_{1/3}Mg_{0.05}O_2$, (*c*)$LiNi_{1/3}Co_{1/3-0.05}Mn_{1/3}Cr_{0.05}O_2$, (*d*) $LiNi_{1/3}Co_{1/3-0.05}Mn_{1/3}Al_{0.05}O_2$

Table 1 Lattice parameters of $LiNi_{1/3}Co_{1/3-x}Mn_{1/3}M_xO_2$ (M = Mg, Cr, Al, x=0, 0.05)

Composition	a/Å	c/Å	c/a	V/Å^3
$LiNi_{1/3}Co_{1/3}Mn_{1/3}O_2$	2.853	14.224	4.986	100.45
$LiNi_{1/3}Co_{1/3-0.05}Mn_{1/3}Mg_{0.05}O_2$	2.861	14.234	4.975	100.88
$LiNi_{1/3}Co_{1/3-0.05}Mn_{1/3}Cr_{0.05}O_2$	2.856	14.227	4.981	100.59
$LiNi_{1/3}Co_{1/3-0.05}Mn_{1/3}Al_{0.05}O_2$	2.851	14.226	4.987	100.49

O_2 (M = Mg, Cr, Al) powders. All the samples show large spherical shapes called secondary particle, and each of the spherical particles is composed of small aggregated primary particles. The size of the secondary particles was varied with different doped elements. The Cr-doped sample showed larger secondary particle than that of the $Li(Ni_{1/3}Co_{1/3}Mn_{1/3})O_2$. The secondary particle size of the Cr-doped sample was about 10 μm, and the undoped sample was only about 5 μm. However, the Mg- and the Al-doped samples exhibited rather smaller secondary particle size compared with the undoped material. The secondary particle size of the Mg- and Al-doped samples was 2~3 μm. Therefore, the incorporation of different elements to $Li(Ni_{1/3}Co_{1/3}Mn_{1/3})O_2$ could affect the particle size of the samples significantly. The Cr-doped materials have the largest particle size, and it may be due to the different doping cations (Mg^{2+}, Cr^{3+}, or Al^{3+}) having various effects on the crystal growing rate of particle during the synthesis process.

In order to further study the influence of the doped elements on the cycling performances of $Li[Ni_{1/3}Mn_{1/3}Co_{1/3}]O_2$ at high voltage up to 4.6 V, the electrochemical performance tests were carried out on the above cathode materials. Figure 3 shows the initial charge and discharge curves of $Li(Ni_{1/3}Co_{1/3}Mn_{1/3})O_2$ and $Li(Ni_{1/3}Co_{1/3-0.05}Mn_{1/3}M_{0.05})O_2$ (M = Mg, Cr, Al) cathodes with a constant current density of 32 mA g^{-1} (0.2 C) between 2.8 and 4.6 V versus Li at room temperature. The first charge capacity and discharge capacity of $Li(Ni_{1/3}Co_{1/3}Mn_{1/3})O_2$ is 207.9 and 173.3 mAh g^{-1}, respectively. The irreversible capacity loss in the first cycle is 34.6 mAh g^{-1} and the coulombic efficiency is 83.4%. As seen from Fig. 3, all doped materials showed lower charge and discharge capacities compared with that of undoped materials. However, all doped materials except the Mg-doped material exhibited higher coulombic efficiency than that of $Li[Ni_{1/3}Mn_{1/3}Co_{1/3}]O_2$. The coulombic efficiencies of Mg-, Cr-, and Al-doped materials at the initial cycling are 78.6%, 95.9%, and 86.6%, respectively.

The higher efficiency of Cr-doped material may be attributed to its low cation mixing according to the XRD results. The integrated intensity ratio of I_{003}/I_{104} (R) is sensitive to the cation mixing [12, 14]. Researchers often

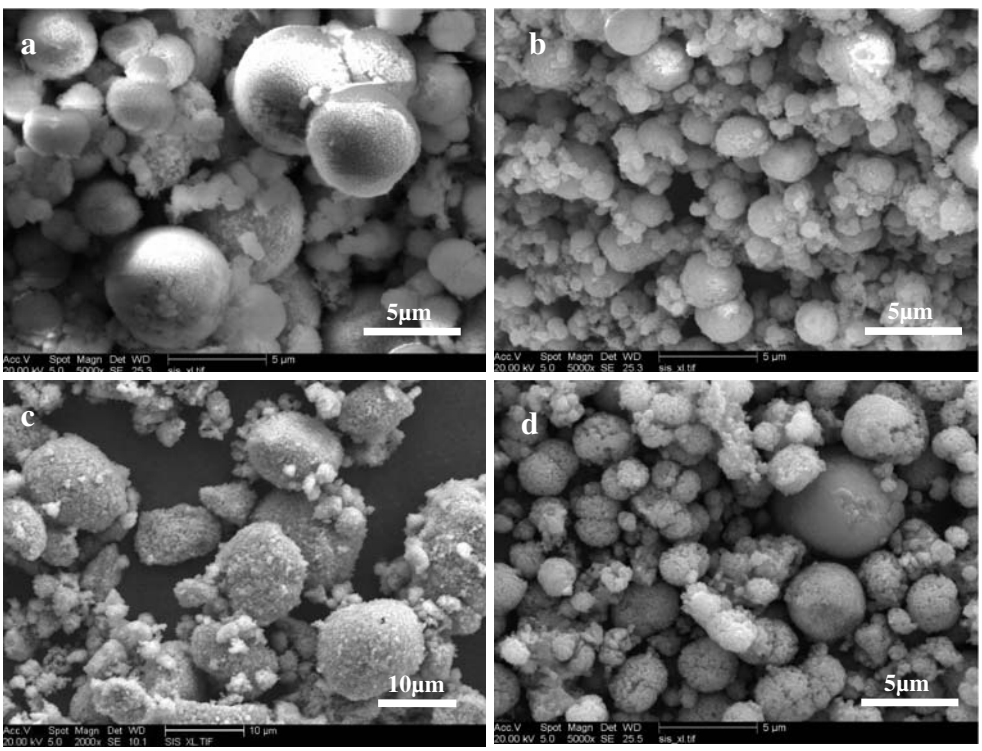

Fig. 2 Scanning electron micrograph of: **a** $Li(Ni_{1/3}Co_{1/3}Mn_{1/3})O_2$ (×5,000), **b** $Li(Ni_{1/3}Co_{1/3-0.05}Mn_{1/3}Mg_{0.05})O_2$ (×5,000), **c** $Li(Ni_{1/3}Co_{1/3-0.05}Mn_{1/3}Cr_{0.05})O_2$ (×2,000), **d** $Li(Ni_{1/3}Co_{1/3-0.05}Mn_{1/3}\ Al_{0.05})O_2$ (×5,000)

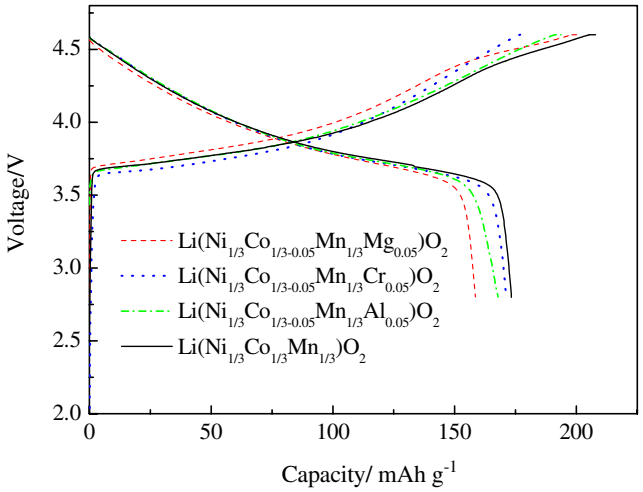

Fig. 3 Voltage profiles of bared and doped $LiNi_{1/3}Co_{1/3}Mn_{1/3}O_2$ electrodes in first cycle at 2.8~4.6 V

used the ratio of I_{003}/I_{104} (R) to indicate the cation mixing of the layered structure [15–18]. Generally, $R<1.2$ is an indication of undesirable cation mixing [19]. We calculated the value of I_{003}/I_{104} from Fig. 1; the value I_{003}/I_{104} of the Cr-doped material (1.29) was higher compared with the undoped material (1.25). However, the value of Mg- and Al-doped materials was lower than that of the undoped material; the value of I_{003}/I_{104} was 1.13 and 1.09, respectively.

Figure 4 compares the cycling performances between $Li(Ni_{1/3}Co_{1/3}Mn_{1/3})O_2$ and $Li(Ni_{1/3}Co_{1/3-0.05}Mn_{1/3}M_{0.05})O_2$ (M = Mg, Cr, Al) operating with a current density of 32 mA g^{-1} between 2.8 and 4.6 V at room temperature. It can be seen that the discharge capacity of the cell $Li(Ni_{1/3}Co_{1/3}Mn_{1/3})O_2$/Li demonstrated a severe capacity fade during cycles. The capacity retention of the undoped material was only 86.6% after 50 cycles. This capacity loss may be caused by the Co dissolution into the electrolyte at higher voltage [20–22]. We can see that the doped materials show different cycling performances; the Cr-doped sample showed no significant capacity fade, and the capacity retention was above 97% after 50 cycles. Oppositely, the materials doped with Mg and Al exhibited an evident capacity fade during cycling; the capacity retention is 82.1% for Mg-doped material and 76.4% for Al-doped material. It can be concluded that Al and Mg doping cannot improve the cycling performance of $Li(Ni_{1/3}Co_{1/3}Mn_{1/3})O_2$ at higher voltage.

The reason for the different capacity retention of the doped and undoped samples is connected with their different particle sizes. As can be seen in Fig. 2, the particle size of the Cr-doped material is about 10 μm, which is larger than that of the undoped sample, and the particle sizes of Mg- and Al-doped samples are smaller than that of the undoped sample. It is known that reducing the particle size and increasing the surface area of the active material can increase its rate capability. However, such an improvement often leads to an increase of undesirable reactions between the electrode and the electrolyte and hence results in the capacity fade. An electrode material with larger particle size is stable because it has a smaller contact area with the electrolyte. The Cr-doped electrodes have the largest particle size. Hence, the cell cycling performance was improved.

Considering the importance of high-power applications, we investigated the effect of doping on the high rate performance. Figure 5 shows the discharge capacities of the electrode with pristine powders and doped powders as active materials at different discharge rates between 2.8 and

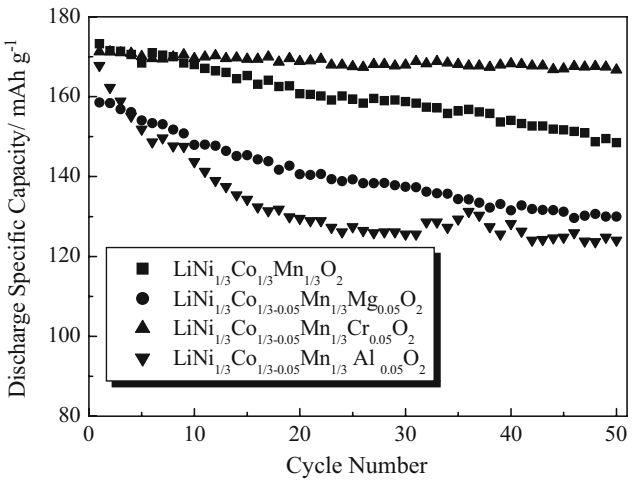

Fig. 4 Cycling performances of bared and doped $LiNi_{1/3}Co_{1/3}Mn_{1/3}O_2$ electrodes at 2.8~4.6 V

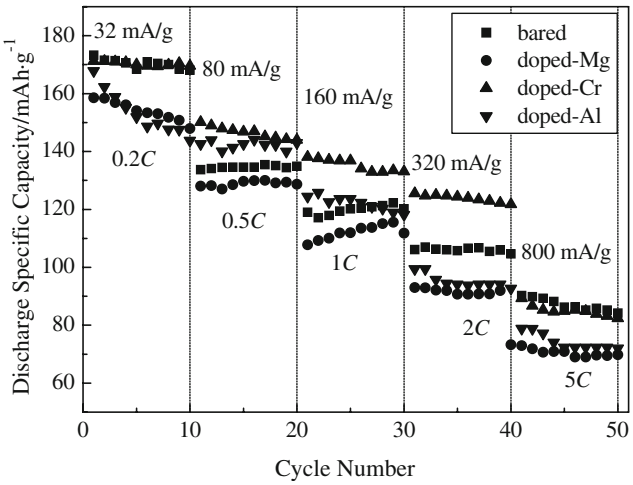

Fig. 5 Rate performances of bared and doped $LiNi_{1/3}Co_{1/3}Mn_{1/3}O_2$ electrodes at 2.8~4.6 V

4.6 V. At low current density (32 and 80 mA g^{-1}), Cr-doped electrode and pristine electrode showed a similar performance. However, the two electrodes showed a large difference in their cycling performance when the current density was increased. The Cr-doped electrode exhibited a higher discharge capacity and better cycling performance than the pristine electrode at 0.5, 1, and 2 C. For example, the Cr-doped electrode delivered a discharge capacity of 125.5 mAh g^{-1} with good cycling performance at 320 mA g^{-1} (2 C), whereas the pristine electrode showed 106.1 mAh g^{-1} at the same current density. The Al-doped electrode exhibited better discharge capacity and cycle stability at 0.5- and 1-C rate, whereas when the rate was up to 2 and 5 C the $LiNi_{1/3}Co_{1/3-0.05}Mn_{1/3}Al_{0.05}O_2$ exhibited a rapid decay in capacity. The Mg-doped electrode exhibited lower discharge capacity than the pristine materials at all discharge rates.

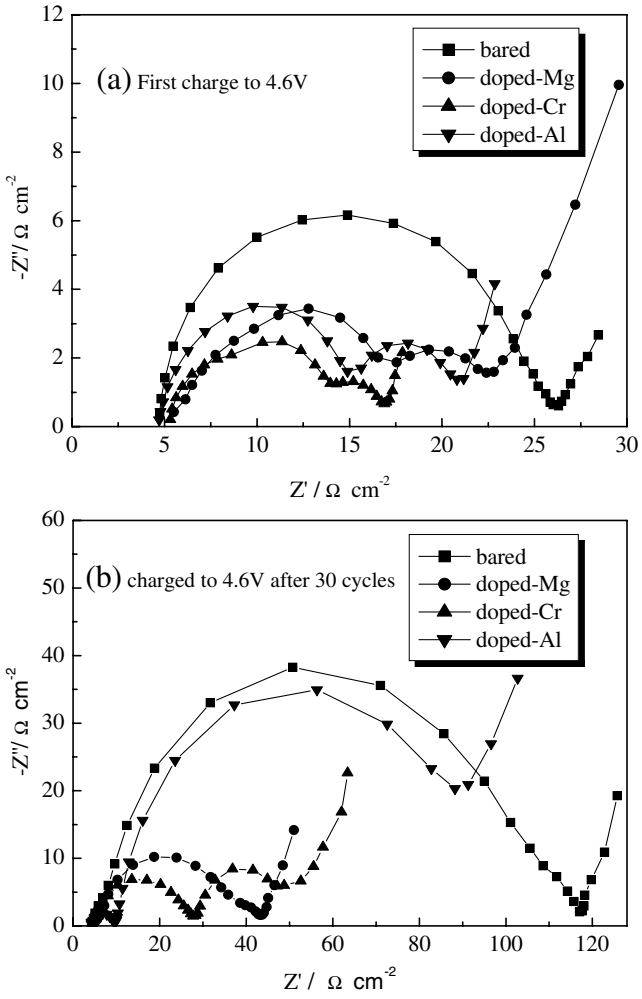

Fig. 6 Nyquist plots of coin cells with bared and doped $LiNi_{1/3}Co_{1/3}Mn_{1/3}O_2$ electrodes: **a** first charge to 4.6 V, **b** charge to 4.6 V after 30 cycles

Table 2 The fitted R_{ct} values of bared and doped $LiNi_{1/3}Co_{1/3}Mn_{1/3}O_2$ electrodes after different cycling numbers

	$R_{ct}/\Omega\ cm^{-2}$			
	Bared	Doped Mg	Doped Cr	Doped Al
1st	25.5	9.88	5.32	6.23
30th	111	60.52	18.88	72.42
30th/1st	4.35	6.13	3.55	11.62

The change of the charge-transfer resistance during cycling was evaluated by EIS. The Nyquist plots of Li $(Ni_{1/3}Co_{1/3-x}Mn_{1/3}M_x)O_2$ (M = Mg, Cr, Al; x=0,0.05) are represented in Fig. 6. All the Nyquist plots are composed of two arcs and a linear. The first arc is associated with the surface film resistance (R_f) owing to passivation layer on the electrode, the second one presents charge-transfer resistance (R_{ct}) associated with the electrochemical process, and the linear is corresponding to diffusion-controlled process in the solid electrode. The impedance spectra of all compounds are fitted to the equivalent circuit with circuit code $R_s(R_fQ)((R_{ct}Z_w)\ Q)$, where R_s is electrolyte resistance, Q is a constant phase element, and Z_w is Warburg impedance.

The fitted values of R_{ct} for all the samples are listed in Table 2. The values of R_{ct} for the doped materials are lower than that of the undoped materials at the initial cycle. After 30 cycles, the values of R_{ct} of the undoped and doped materials all increased. The increscent multiples are 6.13, 3.55, and 11.62 for the Mg-, Cr-, and Al-doped materials, respectively. Among all the doped materials, only the Cr-doped one had the lower increscent multiples than the undoped one. These results indicate that the Cr-doped materials have the best cycling performance at high rate, which can be explained by the suppression of increase of charge-transfer resistance during cycling.

Conclusion

Spherical layered $Li[Mn_{1/3}Ni_{1/3}Co_{1/3}]O_2$ and $Li(Ni_{1/3}Co_{1/3-0.05}Mn_{1/3}M_{0.05})O_2$ (M = Mg, Cr, Al) cathode materials were successfully synthesized by hydroxide coprecipitation method. All the prepared compounds had spherical shapes and the Cr-doped sample had the largest particle size. The XRD results showed that all the samples had well-ordered layered structures with $R3m$ space group. Furthermore, the cycling performance at high voltage (4.6 V) had also been greatly improved by Cr doping; the capacity retention after 50 cycles was above 97%, and it can be attributed to the larger particle size and the prevention of R_{ct} increase during cycling.

References

1. Mizushima K, Jones PC, Wiseman PJ et al (1980) Mater Res Bull 17:783 doi:10.1016/0025-5408(80)90012-4
2. Nagaura T, Tozawa K (1990) Prog Batteries Sol Cells 9:20
3. Chen Y, Wang GX, Konstantinov K et al (2003) J Power Sources 119:184 doi:10.1016/S0378-7753(03)00176-9
4. Ohzuku T, Makimura Y (2001) Chem Lett 30:642 doi:10.1246/cl.2001.642
5. Koyama Y, Tanaka I, Adachi H et al (2003) J Power Sources 119:644 doi:10.1016/S0378-7753(03)00194-0
6. Patoux S, Doeff MM (2004) Electrochem Commun 6:767 doi:10.1016/j.elecom.2004.05.024
7. Andersson AM, Abraham DP, Haasch R et al (2002) J Electrochem Soc 149:A1358 doi:10.1149/1.1505636
8. Amine K, Chen CH, Liu J et al (2001) J Power Sources 97:684 doi:10.1016/S0378-7753(01)00701-7
9. Scrosati B (1995) Nature 373:557 doi:10.1038/373557a0
10. Jouanneau J, Ekerman KW, Krause LJ et al (2003) J Electrochem Soc 150:A1637 doi:10.1149/1.1622956
11. Kim JH, Yoon CY, Sun YK (2003) J Electrochem Soc 150:A158 doi:10.1149/1.1560639
12. Li D, Muta T, Zhang L et al (2004) J Power Sources 132:150 doi:10.1016/j.jpowsour.2004.01.016
13. Luo X, Wang X, Liao L, Gamboa S et al (2006) J Power Sources 158:654 doi:10.1016/j.jpowsour.2005.09.047
14. Ohzuku T, Ueda A, Nagayama M (1993) J Electrochem Soc 140:1862 doi:10.1149/1.2220730
15. Liu ZL, Yu AS, Lee JY (1999) J Power Sources 81:416 doi:10.1016/S0378-7753(99)00221-9
16. Hu SK, Chou TC, Hwang BJ et al (2006) J Power Sources 160:1287 doi:10.1016/j.jpowsour.2006.02.005
17. Oh SW, Park SH, Park CW et al (2004) Solid State Ion 171:167 doi:10.1016/j.ssi.2004.04.012
18. Yabuuchi N, Ohzuku T (2003) J Power Sources 119:171 doi:10.1016/S0378-7753(03)00173-3
19. Luo X, Wang X, Liao L et al (2006) J Power Sources 161:601 doi:10.1016/j.jpowsour.2006.03.090
20. Ye SY, Xia YY, Zhang PW (2007) J Solid State Electrochem 11:805 doi:10.1007/s10008-006-0226-8
21. Myung ST, Lee MH, Komaba S et al (2005) Electrochim Acta 50:4800 doi:10.1016/j.electacta.2005.02.034
22. Sun YK, Han JM, Myung ST et al (2006) Electrochem Commun 8:821 doi:10.1016/j.elecom.2006.03.040